Multiexcitation Fluorescence and Reflectance Spectroscopy as a Real Time Guide to Biopsy in Vivo

Markus G. Müller*[a], Irene Georgakoudi[a], Adam Wax[a], Ramachandra Dasari[a],

Christian Jost[b], Michael Wallace[b], Michael S. Feld[a]

[a]George R. Harrison Spectroscopy Laboratory,

Massachusetts Institute of Technology, Cambridge, MA 02139

[b]Digestive Disease Center, Medical University of South Carolina, Charleston, SC 29425

ABSTRACT

A compact excitation-emission spectrofluorimeter system used to acquire tissue fluorescence and reflectance with fiber optic light delivery and collection is presented. Ten dye cells are pumped by a XeCl excimer laser, creating laser excitation from 308 nm to 505 nm, which is used to excite tissue fluorescence. A xenon-flash lamp is employed to obtain the reflectance spectrum of the corresponding tissue spot. Eleven fluorescence spectra and one white light diffuse reflectance spectrum are collected *in vivo* in 0.2 seconds and can be potentially analyzed in real time to obtain diagnostic information. The instrument can be used for early cancer detection. The measured fluorescence and reflectance spectra are used to model the intrinsic fluorescence of the tissue, which gives important insight into its biochemical composition (tryptophan, collagen, elastin, NADH, etc.) and metabolic state. Diffuse reflectance provides information about tissue morphology, in terms of the scattering and absorption coefficient. By subtracting the diffusely reflected component from the measured reflectance, light scattering spectroscopic (LSS) information due to single backscattering from epithelial cell nuclei can be obtained. LSS provides information about the size distribution of cell nuclei. The parameters give diagnostic information, which can be used to guide the physician in real time while taking biopsies of invisible tissue abnormalities.

Keywords: excitation emission matrix, fluorescence, intrinsic fluorescence, reflectance, spectroscopy, absorption, scattering, light scattering spectroscopy

1. INTRODUCTION

Fluorescence and reflectance spectroscopies are employed by several researchers for cancer and pre-cancer detection [1]. However a phenomenological approach is often used, which does not address the basic chemical and morphological changes in tissue. Additionally, only one or two fluorescence excitation wavelength are usually employed limiting the information obtained. We have designed an instrument, which is a new version of the FastEEM instrument (EEM, excitation-emission-matrix) described previously [2]. This instrument is capable of exciting the tissue with 11 different laser wavelengths (308 nm – 505 nm) and white light. The resulting fluorescence and diffuse reflectance photons are collected in 0.2 seconds, dispersed by a grating and focused on an intensified CCD camera. The data can be potentially analyzed in real time by incorporating analysis software in the Labview-controlled instrument. The system allows the study of tissue fluorescence and reflectance over the entire visible spectrum *in vivo*, and rapid data collection ensures that motion artifacts are negligible. The different excitation wavelengths enable us to

* mmueller@mit.edu; phone: 617-253-6203; fax:617-253-4513

Three-Dimensional and Multidimensional Microscopy: Image Acquisition and Processing VIII,
José-Angel Conchello, Carol J. Cogswell, Tony Wilson, Editors
Proceedings of SPIE Vol. 4261 (2001) © 2001 SPIE. · 0277-786X/00/$15.00

excite several endogenous tissue fluorophores, and allow us to obtain both the emission and excitation spectra. The sensitive ICCD camera and the high laser intensity result in data with very good signal-to-noise ratio (S/N).

To best use the collected data to obtain reliable diagnostic information, we have developed several models that enable us to extract optical tissue parameters such as biochemical composition [3,4] and cell nuclei size distribution [5]. The directly obtained fluorescence can be severely distorted by absorbers such as hemoglobin. This causes wide variations in the observed lineshape and intensity, hindering the interpretation. This effect is especially apparent in the blue region of the spectrum where collagen and NADH fluoresce [3]. Therefore, it is important to extract the intrinsic fluorescence of tissue, which should be a more reliable parameter for a diagnostic decision. The intrinsic fluorescence can be obtained by combining information contained in measured fluorescence and diffuse reflectance from the same tissue spot. The reflectance is acquired over a wide range, 300 nm to 800 nm, in one flash lamp shot. By applying an appropriate model for the diffuse reflectance, we can extract the tissue absorption and reduced scattering coefficient over a wide wavelength range [4]. Additionally, by subtracting the diffusely reflected component from the measured reflectance, light scattering spectroscopic information due to single backscattering from epithelial cell nuclei can be obtained, which can provide information about the size distribution of cell nuclei [5].

2. INSTRUMENTATION

The compact experimental set up is mounted on a movable cart. It consists of a Lambda Physik (Fort Lauderdale, Fl) Optex XeCl excimer laser (308 nm, ~10 mJ, up to 200 Hz repetition rate, pulse duration 10 ns, 7.5mm x 4.5mm beam shape and 2 x 1 mrad beam divergence), ten dye cuvettes (340 nm – 505 nm), a xenon flash lamp L7684 (Hamamatsu Corp., Bridgewater, NJ) (5 μs pulse duration) for white light reflectance (300 nm – 800 nm), an optical fiber bundle to deliver and collect light, a spectrometer with a cooled I-Max 1024 ICCD detector (Princeton Instruments, Trenton, NJ), and a personal computer (Fig. 1). The data acquisition is controlled by Labview (National Instruments, Austin TX) and gives us the capability to incorporate real-time data analysis algorithms. Dye laser wavelengths ranging from 340 nm – 505 nm are produced sequentially by the excimer laser. The high dynamic range in pump energy and, therefore, in dye laser emission (usually only 1-2 mJ of the laser energy is used to pump the dye lasers), results in spectra with good S/N. The dye cuvettes, are mounted on a rotating wheel driven by a motor rotating at 0.2 seconds per cycle. The dye cell wheel rotates and a trigger signal is generated when a dye cell is positioned between a planar output mirror and a concave back mirror (UV-protected aluminum), which form the dye laser cavity.

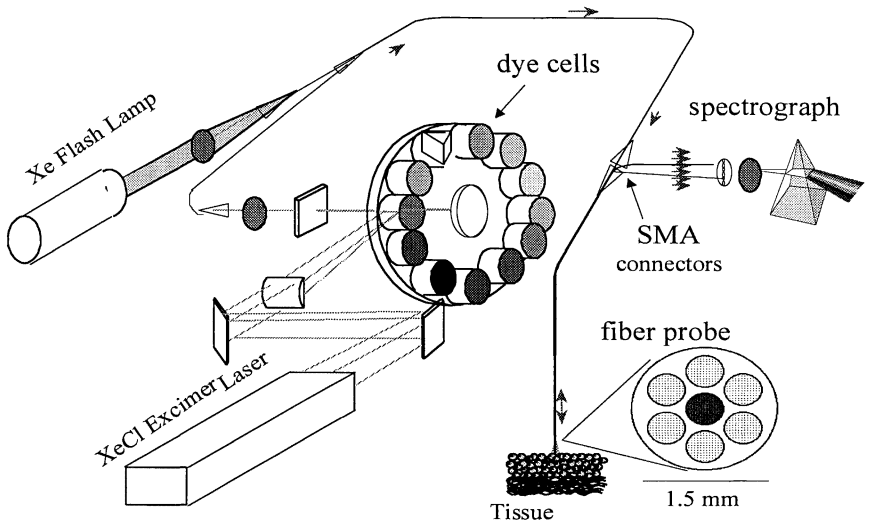

Figure 1: FastEEM instrument.

UV laser excitation wavelengths are limited by the pump beam, which is chosen to operate in a biologically safe wavelength range but still enables us to excite biologically and diagnostically important fluorophores, such as tryptophan [6]. One of the dye cells on the dye wheel is replaced by an optical arrangement consisting of a right-angle prism and a cylindrical lens, which redirects the excimer laser pump light into the same excitation fiber used to deliver the dye laser beams.

The excitation light of the lasers and the flash lamp are coupled into separate fibers, which are fused together to create a fiber optic coupler for two input sources with a single output. The loss in this coupler is smaller than 50%. The single fiber of the coupler is then attached via an SMA connector to the excitation fiber of a 3 m long fiber bundle. The central excitation fiber, for light delivery, is surrounded by six fibers for light collection. At the tip of the fiber probe all seven fibers (200 μm diameter and 0.22 N.A.) are fused together, creating a quartz shield of approximately 1.5 mm diameter. The shield is beveled at a 17° angle and then polished to reduce internal reflections from the boundary between glass and tissue. During each measurement the probe tip is brought into contact with the surface of the sample under investigation, and all spectra are collected from the same spot that was excited. The six collection fibers of the probe are terminated by SMA connectors, which are attached to a fiber bundle guiding the light over a *f*-matched lens to the spectrograph (Acton Research, Spectra Pro 150). The 300 grove/mm grating (blazed at 500 nm) disperses the light on the ICCD. The fiber optic arrangement provides easy maintenance of the system, and the SMA connectors simplify changing the fiber optic probes during consecutive clinical procedures. All fibers used are high OH fibers, and the lenses used are made of fused silica to reduce the UV absorption and to obtain fluorescence (330 nm – 700 nm) and reflectance (300 nm – 800 nm) over a broad wavelength range. FastEEM data acquisition must be rapid to minimize sampling without motion artifacts. The short read-out time of the ICCD and the short time to charge the flash lamp capacitor enable us to collect a full fluorescence EEM and additional white light diffuse reflectance in less than 0.2 sec with high S/N. The S/N is further increased by (Peltier) cooling the intensified CCD to –20 °C. The spectral resolution of the system is determined by the spectrograph entrance slit, the grating, and the detector binning (approximately 7 nm). This resolution is sufficient for examining generally broad fluorescence spectra of human tissue.

3. ANALYSIS MODELS

The large amounts of data obtained can be analyzed using previously described methods: intrinsic fluorescence [3], diffuse reflectance [4] and light scattering spectroscopy [5].

A large variety of endogenous tissue fluorophores can be excited with the FastEEM. Fluorophores such as tryptophan, NADH and FAD are mostly present in the epithelium, and can be distinguished easily by their emission spectra but also by their excitation spectra [1]. For example, tryptophan can only be exited by 308 nm in our system, and NADH fluorescence is strongest at approximately 350 nm excitation. Additional endogenous fluorophores are present in the extracellular matrix; the most prominent are the different types of collagen, a structural protein, which can be excited over the entire wavelength range of our system.

Measured tissue fluorescence spectra are usually not simply linear combinations of spectra of endogenous fluorophores, due to the influence of tissue absorbers and scatterers. This is especially apparent in the blue region of the spectrum, where hemoglobin absorbs strongly and collagen and NADH fluoresce strongly. For this reason, we created a model to extract the intrinsic fluorescence, even when absorption is strong. The model is based on the fact that fluorescence and reflectance, acquired with the same delivery-collection probe geometry, are distorted similarly by scattering and absorption. By using a photon migration picture [3,7], which assumes similar paths for fluorescence and reflectance photons in a turbid medium, the intrinsic fluorescence can be expressed in terms of measured fluorescence and measured diffuse reflectance:

$$f_{xm} = \frac{F_{xm}}{\frac{1}{\mu_{sx} l}\sqrt{\frac{R_{0x}R_{0m}}{\varepsilon_x \varepsilon_m}}\frac{R_x}{R_{0x}}\left(\frac{R_m}{R_{0m}} + \varepsilon_m\right)}} \quad , \tag{1}$$

with f the intrinsic fluorescence, R the reflectance and F the measured fluorescence. The subscripts x and m indicate the dependence of the quantity on excitation and fluorescence emission wavelengths respectively. R_0 is the diffuse reflectance in the absence of absorption. The quantity ε is much smaller than one and given by $\varepsilon = \exp(\beta) - 1$, with $\beta = S(1-g)$ where S is a probe specific parameter and g is the anisotropy coefficient. The intensity of the intrinsic fluorescence is also dependent on the scattering coefficient at the excitation wavelength, μ_{sx}. The quantity l is a constant with dimension of length that characterizes a given light delivery-collection scheme. It can be related to the effective depth from which fluorescence is collected by the probe. This formalism can be used to extract the intrinsic fluorescence from quantities that can be either measured or calculated. For small absorption and small ε, Eq. 1 can be even further simplified and approximated by :

$$f_{xm} \propto F_{xm} / R_m \ . \qquad (2)$$

We note that Eq. 2 , although simple, is not always sufficient to fully remove distortions due to absorption. Eq. 1 was tested with physical tissue models consisting of water, hemoglobin, polystyrene beads and a dye (Furan 2, Lambdachrome). Figure 2 represents the fluorescence spectra of such physical tissue models. It shows the measured fluorescence (hemoglobin, scatterer and a dye present), the measured intrinsic fluorescence (only dye in water) and the modeled intrinsic fluorescence using Eq. 1. All tissue phantoms contain the same amount of dye and are normalized to better visualize the differences in lineshape. The overlap of the modeled and measured intrinsic fluorescence indicates the good performance of the model. The validity of the model has also been tested on tissue and for different excitation wavelengths.

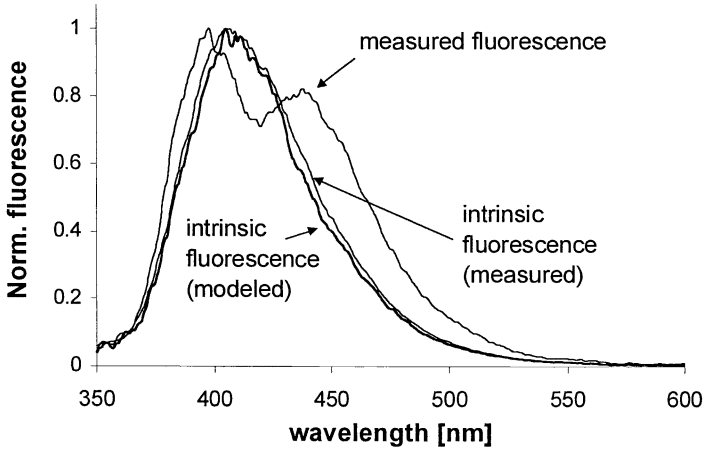

Figure 2: Fluorescence spectra of physical tissue models. One model is a aqueous solution-suspension of hemoglobin 2 g/l, polystyrene beads (0.65% by volume) and a dye. All spectra were excited with 337 nm light of a nitrogen laser.

The absorption coefficient, μ_a, scattering coefficient, μ_s, and anisotropy parameter, g, can be obtained by using a model developed by Zonios *et al.* [4]. This model is based on diffusion theory and enables us to extract the hemoglobin concentration, average scatterer size and density from the measured diffuse reflectance by fitting the model to the experimental data. This gives us additional valuable tissue optical parameters for tissue diagnosis. The model can also be used to analytically obtain the values for R_{0m} and R_{0x} (for $\mu_a = 0$) needed in the extraction of the intrinsic fluorescence in Eq. 1.

Furthermore, we can make use of single scattering from the epithelial-cell nuclei contained in the measured reflectance. However, only a small amount of the incident light is backscattered by the nuclei, and multiple scattering in deeper layers of the tissue randomizes most of the light that is collected. By subtracting the diffuse (randomized) reflected component from the measured reflectance with an appropriate mathematical model, the light scattering spectrum due to single backscattering from epithelial cell nuclei can be extracted [5]. This spectrum can then be compared to Mie theory to provide information about the size distribution of cell nuclei.

3. RESULTS

Fluorescence and reflectance spectra of tissue biochemicals and *in vivo* tissue were obtained with the FastEEM. Figure 3, shows the fluorescence of several biological endogenous fluorophores which can be excited with the system. The fluorophores were dissolved in PBS (1 mM), except for collagen I, which does not dissolve in water/PBS. The small fluorescence in the 700 nm region in the collagen and tryptophan spectra are due to the second order of the grating.

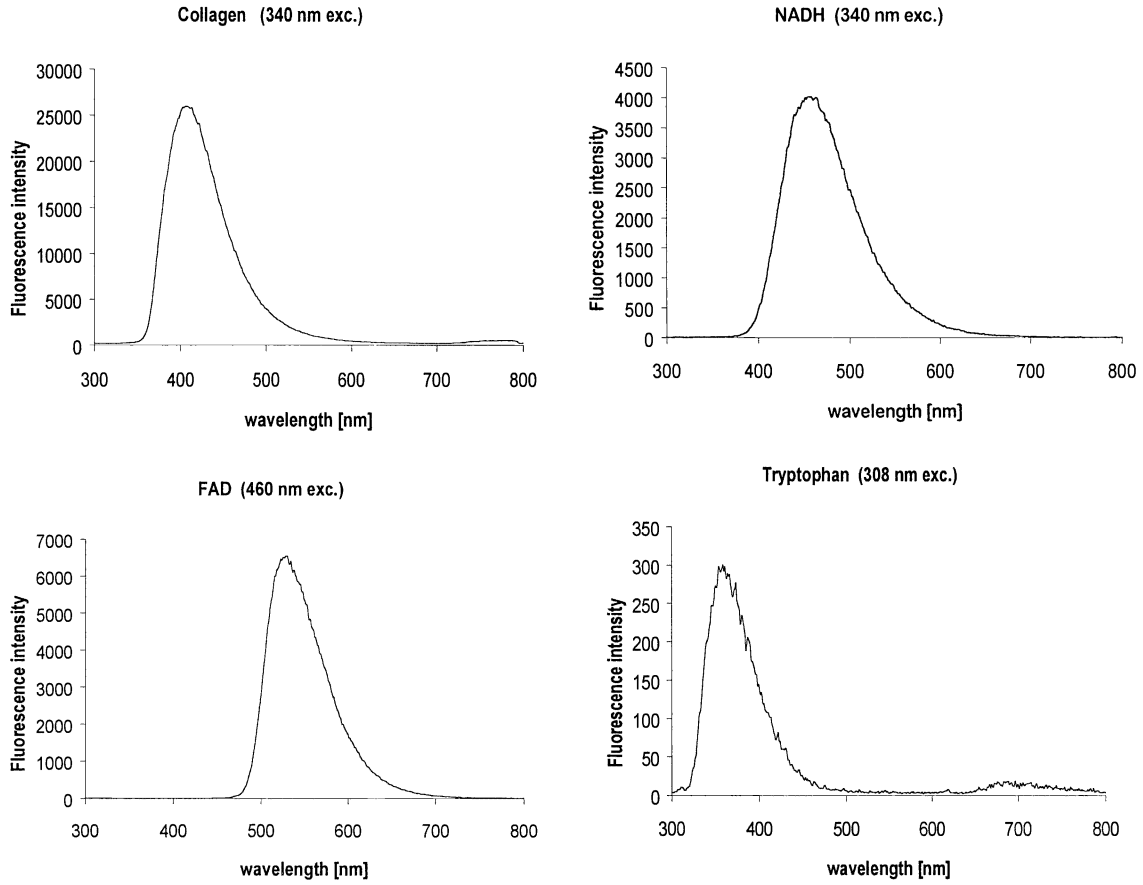

Figure 3: Fluorescence spectra of endogenous tissue fluorophores. The different emission lineshapes and excitation wavelengths are specific to these fluorophores, and can be used to distinguish tissue biochemicals.

All spectra were taken in 1 second as an average over 5 cycles of the dye wheel rotation and by immersing the fiber optic probe in the fluorophore solution/suspension. Fig. 4a shows a fluorescence EEM of colon tissue acquired *in vivo*. The excitation and emission wavelengths are plotted in the x-y plane, and the fluorescence intensity on the z axis. The fiber bundle was inserted through the biopsy channel of an endoscope and the tip of the bundle was brought into gentle contact with the tissue. Using Eq. 1, we can extract the intrinsic colon tissue fluorescence EEM (Fig. 4b). In Figs. 4a and b the differences between the measured fluorescence and intrinsic fluorescence EEM are obvious (dip at 420 nm due to hemoglobin absorption). These distortions are seen frequently in the fluorescence spectrum, which are indicative of the fact that the fluorescence spectra cannot be described as a linear sum of the corresponding spectra of the endogenous tissue fluorophores. Therefore, for accurate analysis it is important to extract the intrinsic

fluorescence. To obtain real-time display of intrinsic fluorescence, the simple approximation of Eq. (2) was incorporated in the data acquisition software. By normalizing the spectra, the lineshapes of different tissue sites can be compared in real time during endoscopy and can help the physician to guide biopsies of tissue abnormalities. Figure 5 shows the output spectra observed on the computer screen during endoscopy at 340 nm excitation. By comparing Fig. 5 to Fig. 2, we see that the normal tissue spectrum is similar to the

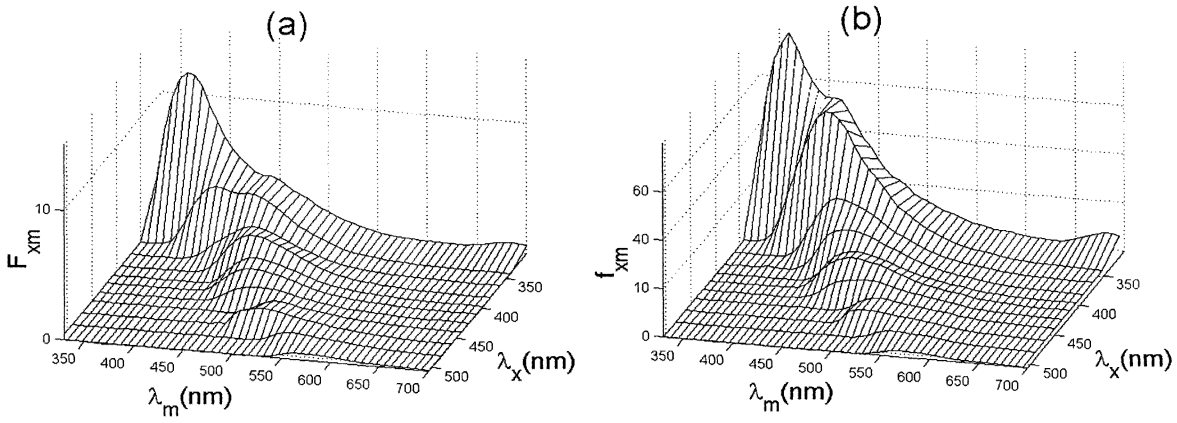

Figure 4: Fluorescence EEM of the measured colon fluorescence *in vivo* (a) and the modeled intrinsic fluorescence (b). In (a) the hemoglobin absorption is visible (λ_m = 420 nm; λ_x = 308 nm, 340 nm, and 362 nm). Tryptophan fluoresces strongest at 308 nm, collagen at all excitation wavelengths.

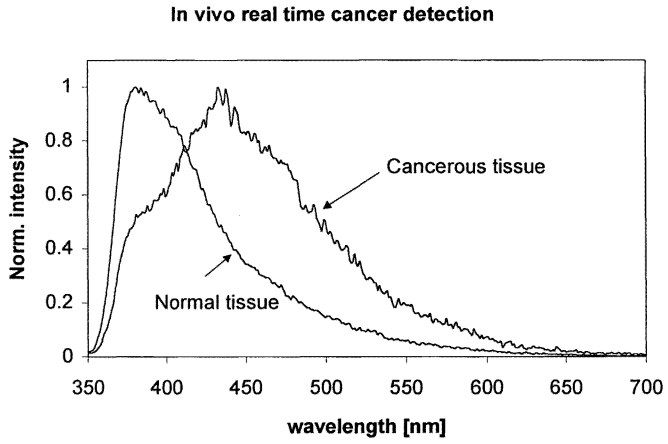

Figure 5: Fluorescence spectra of normal esophageal tissue and squamous cell carcinoma at 340 nm excitation. Shown are approximate normalized intrinsic fluorescence spectra extracted using Eq. 2.

collagen fluorescence spectrum, and that the cancerous tissue spectrum is similar to a combination of NADH and collagen fluorescence spectra (compare lineshapes and peak emissions of collagen ca. 400 nm and NADH ca. 450 nm). This change in fluorescence suggests that NADH is more prominent in cancerous tissue, possibly due to the thicker epithelium and/or higher metabolic activity.

We can also use the measured tissue reflectance spectrum to obtain the tissue absorption coefficient and reduced scattering coefficient, by fitting a diffuse reflectance model to the reflectance data. Figure 6 shows a typical spectrum taken during a GI endoscopic procedure. For this data, we find that $\mu_a = 0.15$ mm^{-1} and $\mu_s' = 2.8$ mm^{-1} at 450 nm. These parameters give valuable information about the scattering behavior of tissue, and the tissue absorber and its concentration (in this case the hemoglobin content). The hemoglobin concentration can be calculated easily by using the well-known oxy- deoxy- hemoglobin extinction coefficients.

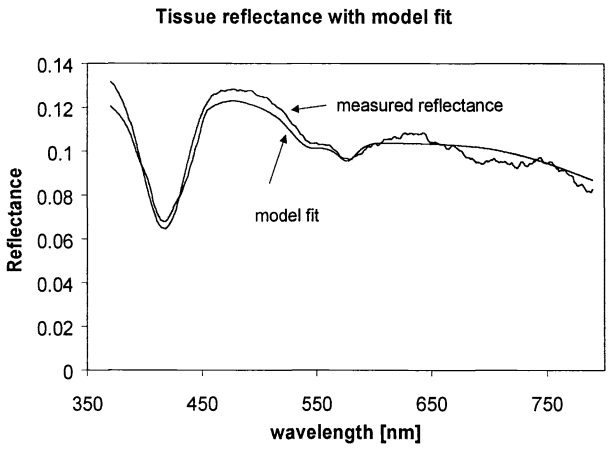

Figure 6: Measured tissue reflectance and diffuse reflectance model fit.

In addition, by subtracting the diffusely reflected component from the measured reflectance in Fig. 6, light scattering spectroscopic information due to single backscattering from epithelial cell nuclei can be obtained providing information about the size distribution of cell nuclei. The result is shown in Fig. 7. The small percentage of enlarged nuclei indicates the absence of dysplastic changes in the cell nuclei of the epithelium.

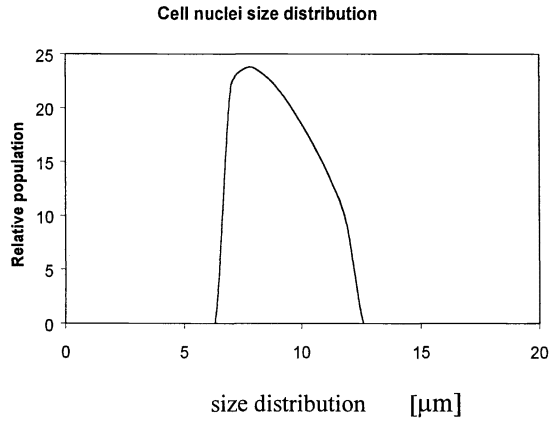

Figure 7: Epithelial cell nuclei size distribution, obtained from the data of Fig. 6. The distribution would broaden and shift to larger size for cancer cells.

4. CONCLUSION

We have described a compact excitation-emission spectrofluorimeter system, which can acquire high quality tissue fluorescence and reflectance spectra with fiber optic light delivery and collection in a short time. We have shown that these spectra can be analyzed to extract intrinsic fluorescence, which provides biochemical information. Furthermore, it is shown that it is feasible to use the intrinsic fluorescence for *in vivo* real time diagnosis of tissue abnormalities. The diffuse reflectance provides scattering and absorption information. In addition, by modeling the diffuse reflectance spectra, light scattering spectra can be obtained, from which the size distribution of epithelial cell nuclei can be extracted. Such information, when provided in real time, can be used as a guide to biopsy of tissue abnormalities.

ACKNOWLEDGEMENTS

We thank Vadim Backman for valuable discussions. This work was carried out at the MIT Laser Biomedical Research Center and was supported by NIH grants P41 RR02594 and R01 CA53717. Irene Georgakoudi is supported by NIH National Research Service Award - 1 F32 CA80345 and Adam Wax is supported by NIH National Research Service Award - 1 F32 RR05075-01.

REFERENCES

1. R. Richards-Kortum and E. Sevick-Muraca, "Quantitative optical spectroscopy for tissue diagnosis," Annual Review of Physical Chemistry **47**, 555-606 (1996).
2. R.A. Zangaro, L. Silveira Jr., R. Manoharan, G. Zonios, I. Itzkan, R.R. Dasari, J. Van Dam, and M.S. Feld, "Rapid multiexcitation fluorescence spectroscopy system for *in vivo* tissue diagnosis," Appl. Opt. **35**, 5211-5219 (1996).
3. Q. Zhang, M.G. Müller, J. Wu, and M.S. Feld, "Turbidity-free fluorescence spectroscopy of biological tissue," Optics Letters **25**, 1451-1453 (2000).
4. G. Zonios, L.T. Perelman, V. Backman, R. Manoharan, M. Fitzmaurice, J. Van Dam, and M.S. Feld, "Diffuse reflectance spectroscopy of human adenomatous colon polyps *in vivo*," Appl. Opt. **38** (31), 6628-6637 (1999).
5. V. Backman, M. Wallace, L. T. Perelman, J. T. Arendt, R. Gurjar, M. G. Müller, Q. Zhang, G. Zonios, E. Kline, T. McGillican, T. Valdez, J. Van Dam, K. Badizadegan, J. M. Crawford, M. Fitzmaurice, S. Kabani, H. S. Levin, M. Seiler, R. R.Dasari, I. Itzkan, and M. S. Feld, "Detection of preinvasive cancer cells," Nature, **406**, 35-36 (2000).
6. M. Anidjar, O. Cussenot, S. Avrillier, D. Ettori, M.J. Villette, J. Fiet, P. Teillac, and A. Le Duc, "Ultraviolet laser-induced autofluorescence distinction between malignant and normal urothelial cells and tissues," Journal of Biomedical Optics **1** (3), 335-341 (1996).
7. J. Wu, M.S. Feld, and R.P. Rava, "Analytical model for extracting intrinsic fluorescence in turbid media," Applied Optics **32** (19), 3585-3595 (1993).